

Contribution from the Department of Chemistry and Biochemistry, James Cook University of North Queensland, Queensland 4811, Australia, and the Department of Chemistry, Polytechnic of North London, London, N7 8DB, United Kingdom

Metal-Ion Recognition. Interaction of O₂N₂-Donor Macrocycles with Cobalt(II), Zinc(II), and Cadmium(II) and Structure of the Zinc Complex of One Such 15-Membered Macrocycle

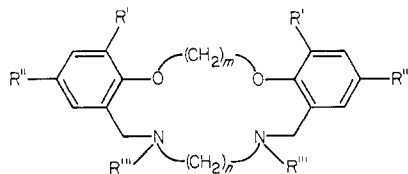
LEONARD F. LINDOY,*^{1a} HYACINTH C. LIP,^{1a} JOHN H. REA,^{1a} ROLAND J. SMITH,^{1a} KIM HENRICK,^{1b} MARY MCPARTLIN,^{1b} and PETER A. TASKER*^{1b}

Received April 10, 1980

Complexes of type M(macrocycle)X₂, where M = Co, Zn, or Cd and X = Cl, Br, I, or NCS, have been synthesized from a range of 14- to 17-membered macrocycles incorporating O₂N₂-donor sets. Physical measurements suggest that the cobalt complexes exhibit either tetrahedral or octahedral geometries. ¹H and ¹³C NMR studies of the zinc and cadmium complexes in dimethyl-*d*₆ sulfoxide indicate that exchange between free and complexed metal ion is fast on the NMR time scale in each case and that the ether donor atoms either are very weakly coordinated or do not coordinate to the metal ion. Stability constants for a number of the zinc complexes in 95% methanol [*I* = 0.1, (CH₃)₄NCl] have been determined potentiometrically and, in contrast to previous studies involving nickel, no well-defined correlation between macrocycle ring size and thermodynamic stability was observed. The X-ray diffraction structure of the zinc iodide complex of one of the 15-membered macrocycles indicates that the two nitrogen donors of the macrocycle together with two iodide ions coordinate to the zinc atom in an approximately tetrahedral arrangement such that the zinc lies outside the cavity of the macrocycle. The ether oxygens of the macrocycle do not coordinate.

Introduction

As part of an overall study of the potential for metal-ion recognition of mixed-donor macrocyclic ligands, synthetic, kinetic, and thermodynamic aspects of the interaction of types 1-7 with nickel(II)²⁻⁵ and copper(II)⁶ have been reported



- 1: R' = R'' = R''' = H, m = n = 2
- 2: R' = R'' = R''' = H, m = 2, n = 3
- 3: R' = R'' = R''' = H, m = n = 3
- 4: R' = R'' = R''' = H, m = 4, n = 3
- 5: R' = OCH₃, R'' = R''' = H, m = 2, n = 3
- 6: R' = H, R'' = Cl, R''' = H, m = 2, n = 3
- 7: R' = H, R'' = H, R''' = CH₃, m = 2, n = 3

recently. X-ray diffraction studies confirm that the nickel ion sits in the hole of the respective 15- and 16-membered macrocycles **2**⁴ and **3**⁵ and a clear correlation between macrocycle hole size and kinetic³ as well as thermodynamic stability⁵ has been observed. Along the 14- to 17-membered unsubstituted ligand series, maximum stability is reached at the 16-membered ring. In contrast, no well-defined relationship between macrocycle ring size and kinetic or thermodynamic stability was observed for copper(II)⁶ where the lack of a ring-size discrimination effect appears largely to reflect the coordination sphere flexibility of this ion. The X-ray structure of the complex (CuLCl)ClO₄ (L = **2**) indicates that the copper ion sits slightly above the hole of the macrocycle which is coordinated in a bent conformation. We now report an extension

of these previous investigations to include a study of the interaction of 1-7 with cobalt(II), zinc(II), and cadmium(II).

Experimental Section

Physical Measurements. ¹H and ¹³C NMR spectra were obtained on a JEOL JHN-MN-100, a JEOL FX60Q, or a Varian XL-100 spectrometer. All chemical shifts are relative to tetramethylsilane. For the NMR titrations, the ligands and metal iodides were dried over P₂O₅ in a vacuum before use; the solid metal salts were added directly to the respective ligand solutions (~0.05 M) in 0.5 mL of hexadeuteriodimethyl sulfoxide (Me₂SO-*d*₆) contained in the NMR tube.

The stability constant determinations were obtained potentiometrically, under conditions identical with those described previously,^{5,6} by using solutions of the respective solid complexes. The complexes were dissolved in 95% methanol which was 4 × 10⁻³ M in HCl (*I* = 0.1, (CH₃)₄NCl) to yield solutions which were 2 × 10⁻³ M in complex. These were titrated with 0.1 M (CH₃)₄NOH under a stream of methanol-saturated nitrogen. Quoted log *K* values are the weighted mean from two or three separate titrations. Other physical measurements were obtained as previously described.²

Synthesis of the Complexes. Zinc and Cadmium Complexes of Type M(macrocycle)X₂ (M = Zn, Cd; X = Cl, I). Macrocycle (0.002 mol) in dry methanol or methanol/chloroform (20 mL) was added dropwise to a stirred, boiling solution of metal halide (0.002 mol) in dry methanol or methanol/chloroform (50 mL). The product was washed with methanol and dried under vacuum over P₂O₅; yield 60-90%.

Cobalt(II) Complexes of Type Co(macrocycle)X₂ (X = Cl, Br, NCS). By a similar procedure to that used for the zinc and cadmium complexes, a mixture of the macrocycle and the cobalt(II) salt in butanol yielded the respective cobalt complexes; yield 40-80%.

X-ray Crystallography. Crystal data for ZnL₂, L = **7**: C₂₁H₂₈I₂N₂O₂Zn, mol wt 659.4, triclinic,⁷ space group C1, *a* = 22.209 (3) Å, *b* = 12.251 (5) Å, *c* = 8.932 (2) Å, α = 101.00 (3)°, β = 91.68 (4)°, γ = 89.53 (5)°, *V* = 2384.5 Å³, *T* = 22 °C, *d*(calcd) = 1.836 g cm⁻³, *Z* = 4, μ(Mo Kα) = 34.3 cm⁻¹. The centric space group⁷ was assumed and subsequently confirmed by the satisfactory refinement of the structure.

Data were collected on a crystal of dimensions ca. 0.20 × 0.15 × 0.12 mm by using a Philips PW1100 four-circle diffractometer and graphite-monochromatized Mo Kα radiation (λ = 0.7107 Å). The ω-2θ scan mode was used, and reflections with 3.0° < θ < 25.0° in one hemisphere were examined. Most intensities were measured more than once: weak reflections which gave *I*_i - 2*I*_i^{1/2} < *I*₀ on a preliminary scan were not further examined (*I*_i is the count rate at the top of the

- (1) (a) James Cook University of North Queensland. (b) Polytechnic of North London.
- (2) Armstrong, L. G.; Grimsley, P. G.; Lindoy, L. F.; Lip, H. C.; Norris, V. A.; Smith, R. J. *Inorg. Chem.* **1978**, *17*, 2350.
- (3) Ekstrom, A.; Lindoy, L. F.; Smith, R. J. *J. Am. Chem. Soc.* **1979**, *101*, 4014. Ekstrom, A.; Lindoy, L. F.; Smith, R. J. *Inorg. Chem.* **1980**, *19*, 724.
- (4) Ekstrom, A.; Lindoy, L. F.; Lip, H. C.; Smith, R. J.; Goodwin, H. J.; McPartlin, M.; Tasker, P. A. *J. Chem. Soc., Dalton Trans.* **1979**, 1027.
- (5) Adam, K. R.; Lindoy, L. F.; Smith, R. J.; Anderegg, G.; Henrick, K.; McPartlin, M.; Tasker, P. A. *J. Chem. Soc., Chem. Commun.* **1979**, 812. Anderegg, G.; Ekstrom, A.; Lindoy, L. F.; Smith, R. J. *J. Am. Chem. Soc.* **1980**, *102*, 2670.
- (6) Adam, K. R.; Anderegg, G.; Lindoy, L. F.; Lip, H. C.; McPartlin, M.; Rea, J. H.; Smith, R. J.; Tasker, P. A. *Inorg. Chem.* **1980**, *19*, 2956.

- (7) The standard primitive cell has *a* = 12.687 Å, *b* = 12.251 Å, *c* = 8.932 Å, α = 101.00°, β = 86.20°, and γ = 118.40°. The C1 cell was used in refinement to prevent correlations due to the large γ value. Unit cell parameters were obtained from a least-squares fit of the setting angles of 25 reflections with 2θ values ca. 20°.

Table I. Refined Atomic Positional and Isotropic Thermal Parameters

atom	x ^a	y	z	U ^b
Zn	5974 (1)	3732 (1)	1628 (2)	
I(1)	6172 (1)	3172 (1)	-1216 (1)	
I(2)	6200 (1)	5773 (1)	2813 (1)	
O(1a)	4808 (5)	448 (10)	2227 (19)	
O(1b)	5863 (5)	-5 (8)	3527 (20)	
N(1a)	5079 (5)	3399 (9)	2123 (12)	52 (3)
N(1b)	6461 (5)	2673 (8)	2825 (11)	48 (3)
C(1a)	4871 (7)	-505 (12)	2675 (18)	
C(2a)	4264 (7)	885 (12)	1958 (17)	63 (4)
C(3a)	3731 (8)	379 (14)	2177 (19)	84 (5)
C(4a)	3193 (8)	901 (14)	1797 (19)	80 (5)
C(5a)	3181 (8)	1812 (15)	1185 (20)	89 (5)
C(6a)	3734 (7)	2297 (14)	918 (18)	79 (5)
C(7a)	4275 (6)	1856 (11)	1371 (15)	55 (4)
C(8a)	4873 (6)	2357 (11)	1047 (15)	57 (4)
C(9a)	5081 (7)	3303 (12)	3767 (16)	62 (4)
C(10a)	4677 (7)	4366 (12)	1912 (17)	66 (4)
C(1b)	5498 (7)	-828 (11)	2852 (18)	
C(2b)	6467 (7)	-123 (12)	3326 (16)	63 (4)
C(3b)	6769 (8)	-919 (14)	3942 (18)	77 (5)
C(4b)	7389 (8)	-1027 (15)	3871 (20)	85 (5)
C(5b)	7701 (8)	-340 (14)	3150 (19)	80 (5)
C(6b)	7401 (7)	489 (13)	2524 (17)	70 (4)
C(7b)	6784 (6)	622 (10)	2651 (14)	45 (3)
C(8b)	6462 (6)	1492 (11)	1905 (15)	58 (4)
C(9b)	6184 (6)	2761 (13)	4324 (17)	67 (4)
C(10b)	7099 (7)	3093 (12)	3039 (17)	67 (4)
C(9c)	5503 (6)	2505 (12)	4289 (17)	67 (4)

^a Fractional coordinates $\times 10^4$ for the $C\bar{1}$ cell.⁷ The standard deviation of the least significant digit is included in parentheses in this and subsequent tables. ^b Isotropic thermal parameters $\times 10^3$ in \AA^2 . Anisotropic thermal parameters are given in Table II.

reflection peak and I_b is the mean of the count rate for two preliminary 5-s background measurements on either side of the peak). Of the remaining 2355 reflections, those for which the total intensity recorded in the first scan of the peak (I_1) was <500 , counts were scanned twice to increase their accuracy. A constant scan speed of $0.05^\circ/\text{s}$ and a scan width of 1.10° were used, with a background-measuring time proportional to I_b/I_1 . Three standard reflections were measured every 3 h during data collection and showed no significant variations in intensity.

The reflection intensities were calculated from the peak and background measurements by using a program⁸ written for the PW1100 diffractometer. The variance of intensity, I , was calculated as $\{[\sigma_c(I)]^2 + (0.04I)^2\}^{1/2}$, where $\sigma_c(I)$ is the variance due to counting statistics and the term in I^2 was introduced⁹ to allow for other sources of error. I and $\sigma(I)$ were corrected for Lorentz and polarization factors, and a semiempirical absorption correction based on a pseudoellipsoid model¹⁰ was made. A total of 324 azimuthal scan data from 14 independent reflections were used; relative transmission factors ranged from 0.681 to 0.836, and for the full data set the merging R factor based on equivalent reflections was 0.044 before correction and 0.011 after correction. Reflections for which $I < 3\sigma(I)$ were rejected, and equivalent reflections were averaged to give 2020 unique reflections.

Structure Solution and Refinement. The zinc and two iodine atoms were located from a Patterson map. Least-squares refinement of their positional and isotropic thermal parameters gave $R = 0.251$. A subsequent difference Fourier synthesis revealed the positions of all the remaining nonhydrogen atoms. Refinement with isotropic thermal parameters for all atoms converged at $R = 0.119$. In the final cycles of refinement anisotropic thermal parameters were assigned to Zn, I, and O atoms and the atoms C(1a) and C(1b), where for the two C atoms higher isotropic thermal parameters were found. Hydrogen atoms were included in calculated positions, "riding" at a fixed distance of 1.08 \AA from the carbon atoms to which they were attached and

Table II. Anisotropic Thermal Parameters (\AA^2) $\times 10^3$

atom	U ₁₁ ^a	U ₂₂	U ₃₃	U ₁₂	U ₁₃	U ₂₃
Zn ^b	596 (11)	365 (8)	441 (9)	13 (7)	32 (8)	107 (7)
I(1) ^b	668 (7)	581 (6)	428 (5)	-79 (5)	97 (5)	140 (4)
I(2) ^b	913 (9)	361 (5)	833 (8)	-36 (5)	-36 (6)	48 (5)
O(1a)	66 (9)	79 (8)	248 (18)	-27 (7)	-52 (9)	88 (10)
O(1b)	50 (7)	45 (7)	263 (18)	6 (6)	15 (9)	28 (9)
C(1a)	56 (11)	51 (9)	84 (11)	-14 (8)	17 (9)	0 (8)
C(1b)	68 (11)	41 (8)	88 (11)	-17 (8)	-7 (9)	17 (8)

^a Expressed in the form $\exp[-2\pi^2(U_{11}h^2a^{*2} + U_{22}k^2b^{*2} + U_{33}l^2c^{*2} + 2U_{12}hka^*b^* + 2U_{13}hla^*c^* + 2U_{23}klb^*c^*)]$. ^b The values for the Zn and I atoms are given $\times 10^4$.

Table III. Magnetic, Infrared, and Visible (Solid State) Spectral Data for the Cobalt(II) Complexes

compd (color)	μ_e ^a , μ_B	$\nu(\text{NCS})$, cm^{-1}	λ_{max} , nm
CoL(SCN) ₂ , L = 2 (pink)	4.76	2075, 2055	500, 550
CoLBr ₂ ·H ₂ O, L = 2 (pink)	5.18		485, 520, 540, 575
CoL(SCN) ₂ , L = 3 (purple)	5.01	2090, 2065	500, 525, 565
CoL(SCN) ₂ , L = 4 (blue)	4.44	2065	560, 590, 620
CoLBr ₂ , L = 4 (blue)	4.52		600, 625, 640
CoLCl ₂ , L = 4 (blue)	4.39		560, 610, 630

^a At 24 °C.

having a common isotropic thermal parameter ($=0.107$ (11) \AA^2). This resulted in $R = 0.0483$ and $R_w = 0.0505$ [where $R_w = \sum |F_o| - |F_c|/|w|^{1/2} / \sum |F_o|/|w|^{1/2}$ and weights (w) were assigned to reflections as $w = 1/\sigma^2(F_o)$]; maximum shift = 0.014 σ and average shift = 0.006 σ . The final difference Fourier map showed maxima and minima of electron density of 0.96 and -0.79 e \AA^{-3} , respectively, in regions close to the iodine atoms.

Major computations were performed by using the SHELX programs.¹¹ Scattering factors and anomalous dispersion corrections were taken from ref 12 and 13.

Atomic positional and thermal parameters are given in Tables I and II.

Results and Discussion

Synthesis and Characterization of the Complexes. Zinc complexes of type Zn(macrocycle) X_2 (where macrocycle = 1-7 and X = I; macrocycle = 2, 4, or 7 and X = Cl) as well as cadmium complexes of type Cd(macrocycle) I_2 (where macrocycle = 2-6) have been isolated and characterized as white or off-white solids. Cobalt(II) complexes (which proved somewhat more difficult to isolate than the zinc or cadmium complexes) of type Co(macrocycle) X_2 (macrocycle = 2-4, X = NCS; macrocycle = 2 or 4, X = Br; macrocycle = 4, X = Cl) were obtained.

The complexes generally display low solubilities in organic solvents, and it was only possible to use a selection of the most soluble complexes for subsequent comparative solution studies. All the complexes (with the exception of those of the N-dimethylated derivative 7) yielded infrared absorptions in the range 3300-3170 cm^{-1} which arose from the $\nu(\text{N-H})$ modes of the coordinated ligand. Where soluble, the complexes showed only small conductances (considerably less than the value expected for a 1:1 complex in each case) in acetonitrile or nitrobenzene (at 25 °C)¹⁴ and this is thus consistent with the anions being largely coordinated to the metal ion in these solvents. In accord with the greater ionizing ability of dimethyl sulfoxide, conductances in this solvent were higher and yielded values which generally fell between those expected for 1:1 and 2:1 electrolytes.

- (8) Hornstra, J.; Stubbe, B. "PW1100 Data Processing Program (DRED)"; Philips Research Laboratories: Eindhoven, The Netherlands, 1972.
 (9) Corfield, P. W. R.; Doedens, R. J.; Ibers, J. A. *Inorg. Chem.* **1967**, *6*, 197.
 (10) Sheldrick, G. M. "EMPABS Program"; University Chemical Laboratory: Cambridge, U.K., 1976.

- (11) Sheldrick, G. M. "SHELX-76 Program System"; University Chemical Laboratory: Cambridge, U.K., 1976.
 (12) Doyle, P. A.; Turner, P. S. *Acta Crystallogr., Sect. A* **1968**, *A24*, 390.
 (13) Cromer, D. T.; Liberman, D. J. *Chem. Phys.* **1970**, *53*, 1891.
 (14) Geary, W. J. *Coord. Chem. Rev.* **1971**, *7*, 81.

All the cobalt complexes are high spin (Table III). High-spin cobalt(II) complexes commonly have either tetrahedral or octahedral stereochemistries although five-coordinate complexes also occur.¹⁵ Tetrahedral complexes normally exhibit absorption bands in the 600–700-nm region of the visible spectrum (and are typically deep blue or green) with magnetic moments in the range 4.4–4.8 μ_B .¹⁶

Octahedral complexes usually display bands below about 600 nm in their visible spectra (the color is typically lilac or pink) and give magnetic moments in the range 4.7–5.2 μ_B .¹⁶ The magnetic moments (Table III) and visible reflectance spectra (Table III) are thus consistent with the cobalt complexes of **4** having tetrahedral geometries whereas the remaining complexes appear octahedral. The conductance values taken together with the infrared $\nu(\text{NCS})$ values (Table III) for the respective thiocyanate complexes, which fall in the region expected for N-bonded thiocyanato ligands,¹⁷ suggest that the anions are coordinated in the solid state in each of the complexes.¹⁸

In the absence of X-ray diffraction studies on these complexes, absolute assignment of their stereochemistries cannot be made; however, from the above data it appears likely that the complexes of **4** are tetrahedral whereas the complexes of the other two ligands are octahedral or pseudooctahedral. Thus for the tetrahedral species the evidence implies that two of the donor atoms (presumably the ether oxygens) of the macrocycle do not coordinate; such noncoordination is likely to be facilitated for **4** as it consists of the largest (most flexible) ring of this series of macrocycles. The noncoordination of the ether linkages to copper in complexes of macrocyclic ligands incorporating both ether oxygen and nitrogen heteroatoms has been confirmed recently for three such complexes by X-ray diffraction.^{19,20}

NMR Studies Involving the Zinc and Cadmium Complexes.

For investigation of the nature of the zinc and cadmium complexes in solution, ¹H and ¹³C NMR studies were undertaken in Me₂SO-*d*₆. For selected ligands, incremental addition of zinc or cadmium iodide was found to lead to small shifts in the respective resonances.²¹ Thus, in contrast to the usual kinetic inertness of many macrocyclic systems,²² the present complexes are kinetically labile as evidenced by the averaging of the free and complexed ligand signals. Provided only 1:1 metal ligand complexes are formed, the observed chemical shift (δ) of a ligand proton will be the weighted average of the proton in the free and complexed ligands (δ_f and δ_c , respectively)²³ as in eq 1 where [L₀] is the initial

$$\delta_{\text{obsd}} = \frac{[\text{L}_0] - [\text{ML}]}{[\text{L}_0]} \delta_f + \frac{[\text{ML}]}{[\text{L}_0]} \delta_c \quad (1)$$

- (15) Carlin, R. L. *Transition Met. Chem. (N.Y.)* **1965**, *1*, 1.
 (16) Cotton, F. A.; Wilkinson, G. "Advanced Inorganic Chemistry, A Comprehensive Text", 3rd ed.; Wiley: New York, 1972. Figgis, B. N.; Lewis, J. *Prog. Inorg. Chem.* **1964**, *6*, 185.
 (17) Lewis, J.; Nyholm, R. S.; Smith, P. W. J. *Chem. Soc.* **1961**, 4590. Burmeister, J. L. *Coord. Chem. Rev.* **1968**, *3*, 225.
 (18) The C–S stretching mode is obscured by ligand bands in each of the complexes.
 (19) Herceg, M.; Weiss, R. *Inorg. Nucl. Chem. Lett.* **1970**, *6*, 435. Drew, M. G. B.; McCann, M.; Nelson, S. M. *J. Chem. Soc., Chem. Commun.* **1979**, 481.
 (20) Adam, K. R.; Lindoy, L. F.; Lip, H. C.; Rea, J. H.; Skelton, B. W.; White, A. H. *J. Chem. Soc., Dalton Trans.*, in press.
 (21) It has been well documented that coordination of macrocycles to diamagnetic ions generally leads to only small chemical shifts; see for example: Knochel, A.; Klimes, J.; Oehler, J.; Rudolph, G. *Inorg. Nucl. Chem. Lett.* **1975**, *11*, 787. Lehn, J. M.; Simon, J. *Helv. Chim. Acta* **1977**, *60*, 141. Knochel, A.; Oehler, J.; Rudolph, G.; Sinnwell, V. *Tetrahedron* **1977**, *33*, 119. Lockhart, J. C.; Robson, A. C.; Thompson, M. E.; Tyson, P. D.; Wallace, I. H. M. *J. Chem. Soc., Dalton Trans.* **1978**, 611.
 (22) Lindoy, L. F. *Chem. Soc. Rev.* **1975**, *4*, 421. Margerum, D. W.; Cayley, G. R.; Weatherburn, D. C.; Pagenkopf, G. K. *ACS Monogr.* **1978**, No. 174.

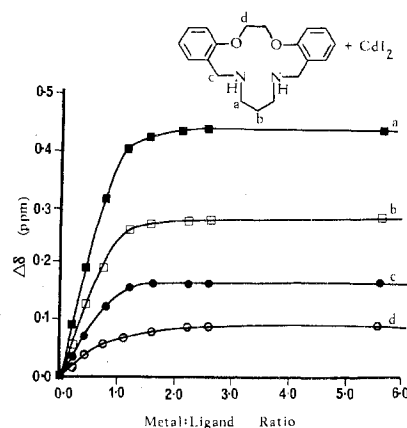


Figure 1. Effect of incremental addition of cadmium iodide on the aliphatic proton resonances of ligand **2** (concentration 0.05 M) in Me₂SO-*d*₆.

Table IV. Induced ¹H NMR Chemical Shifts ($\Delta\delta$) on Complexation of the O₂N₂-Donor Macrocycles to Zinc(II) and Cadmium(II) in Me₂SO-*d*₆

macrocycle	$\Delta\delta^a$	
	OCH ₂	NCH ₂ , arom-CH ₂ N
	Zn(macrocycle)I ₂	
1	-0.08	+0.16, -0.35
2	-0.09	-0.46, -0.26
3	-0.05	-0.49, -0.58
4	-0.02	-0.28, ?
7	-0.07	-0.23, -0.23
	Cd(macrocycle)I ₂	
1	-0.06	+0.16, -0.28
2	-0.08	-0.40, -0.16
3	-0.04	-0.42, -0.30
4	-0.08	-0.24, -0.23

^a A negative value indicates a shift to lower field.

concentration of the ligand and [ML] is the equilibrium concentration of the metal complex. The relatively high stabilities of the present complexes ($K > 10^3 \text{ mol}^{-1}$) resulted in attempts to calculate stability constants by this method being unsuccessful. However, the stoichiometries of metal complex formation were obtained by plotting the shifts of the ligand proton resonance positions as a function of metal-ion concentration. The effects of incremental addition of zinc or cadmium iodide on the ¹H NMR spectra of ligands **2**, **3**, and **5** were all qualitatively similar; the sole formation of a 1:1 (metal:ligand) species was observed in each case. A typical plot (addition of cadmium iodide to **2** in Me₂SO-*d*₆) is reproduced in Figure 1. For this and the other systems studied, insignificant shifts occurred for the aromatic proton resonances. A feature of all the titrations is the very small induced shifts for the methylene protons which are adjacent to the ether functions. In contrast, greater $\Delta\delta$ values were observed for protons adjacent to the nitrogen donor atoms. In view of this, the NMR spectra of an extended range of zinc and cadmium iodide complexes were obtained in Me₂SO-*d*₆ and the respective chemical shifts compared with those of the free macrocycles under similar conditions. Table IV summarizes the $\Delta\delta$ values for the respective (aliphatic) protons. Once again the resonances for protons adjacent to the oxygen atoms undergo quite small shifts. These results suggest that coordination of the nitrogen atoms of the respective macrocycles to zinc and cadmium occurs, while any metal ion–oxygen interaction is either weak or nonexistent. It is significant in this

- (23) Kan, L. S.; Li, N. C. *J. Am. Chem. Soc.* **1970**, *92*, 4823. Wang, S. M.; Li, N. C. *Ibid.* **1968**, *90*, 5069.

Table V. ¹H NMR Assignments^{a,b} for Selected Macrocycles and Their Zinc and Cadmium Complexes in Me₂SO-d₆

compd	δ			
	OCH ₂	NCH ₂ CH ₂ , arom-CH ₂ N	NCH ₂ CH ₂ , OCH ₂ CH ₂	aromatic
ligand 1	4.33 (s)	2.60 (s), 3.60 (s)		6.85-7.40 (m)
ZnLI ₂ (L = 1)	4.41 (s)	2.44 (s), 3.95 (s)		6.95-7.54 (m)
CdLI ₂ (L = 1)	4.39 (s)	2.44 (s), 3.88 (s)		6.84-7.43 (m)
ligand 2	4.34 (s)	2.50 (t), 3.59 (s)	1.54 (m)	6.77-7.36 (m)
ZnLI ₂ (L = 2)	4.43 (s)	2.96 (b, t), 3.85 (s)	1.91 (b)	6.86-7.47 (m)
CdLI ₂ (L = 2)	4.42 (s)	2.90 (t), 3.75 (s)	1.78 (q)	6.91-7.35 (m)
ligand 3	4.20 (t)	2.20 (t), 3.61 (s)	1.46 (q), 2.20 (q)	6.81-7.23 (m)
ZnLI ₂ (L = 3)	4.25 (b)	2.69 (b), 4.19	1.6 (b), 2.28 (b)	6.88-7.56 (m)
CdLI ₂ (L = 3)	4.24 (t)	2.62 (t), 3.91 (s)	1.62 (b), 2.24 (q)	6.92-7.37 (m)
ligand 4	4.04 (b)	2.54 (t), 3.64 (s)	1.59 (q), 1.95 (b)	6.75-7.33 (m)
ZnLI ₂ (L = 4)	4.06 (b)	2.82 (b), (?)	1.9 (sh, b), 2.04 (b)	6.91-7.52 (m)
CdLI ₂ (L = 4)	4.12 (b)	2.78 (b), 3.87 (b)	1.8 (b), 2.03 (b)	6.93-7.37 (m)
ligand 7 ^c	4.27 (s)	2.38 (t), 3.48 (s)	1.42 (q)	6.77-7.34 (m)
ZnLI ₂ (L = 7) ^d	4.34 (s)	2.61 (t), 3.71 (s)	1.60 (b)	6.83-7.44 (m)

^a In ppm relative to tetramethylsilane. ^b s = singlet, t = triplet, q = quintet, m = multiplet, b = broad. ^c Contains N-CH₃ resonance at 2.01 ppm (s). ^d Contains N-CH₃ resonance at 2.18 ppm (s).

Table VI. ¹³C NMR Assignments^{a,b} for Selected Macrocycles and Their Zinc and Cadmium Complexes in Me₂SO-d₆

compd	δ			
	OCH ₂	NCH ₂ CH ₂ , arom-CH ₂ N	NCH ₂ CH ₂ , OCH ₂ CH ₂	aromatic
ligand 1	66.5	47.2, 48.9		112.3, 120.5, 128.2, 129.0, 130.5, 156.6
ZnLI ₂ (L = 1)	65.9	42.0, 45.3		112.5, 121.0, 124.8, 129.2, 131.2, 156.0
CdLI ₂ (L = 1)	65.7	42.4, 45.3		112.3, 120.9, 126.2, 128.6, 130.9, 155.8
ligand 2	65.5	47.8, ^c 50.4 ^c	28.9	110.5, 119.7, 128.0, 128.1, 130.5, 156.5
ZnLI ₂ (L = 2)	65.4	47.4 (b), ^d 48.9	23.0 (b)	111.8, 120.2, 123.5, 129.4, 131.4, 156.3
CdLI ₂ (L = 2)	65.7	47.9, 48.5	25.6	111.4, 120.0, 125.6, 128.9, 131.1, 156.2
ligand 3	65.9	46.9, 48.5	29.4, 28.8	113.9, 120.7, 127.9, 129.7, 130.3, 156.8
ZnLI ₂ (L = 3)	68.0	43.9 (b), 44.6	29.2, 19.0 (b)	111.8, 120.5, 122.8, 129.1, 130.2, 157.1
CdLI ₂ (L = 3)	67.3	45.9, 46.2	29.3, 23.6	112.8, 120.6, 126.0, 128.6, 130.2, 156.9
ligand 4	66.7	46.9, 48.8	29.5, 25.7	111.1, 119.9, 128.0, 128.5, 130.3, 156.8
ZnLI ₂ (L = 4)	67.1	43.7 (?), 46.1	30.6, 25.8	111.4, 120.2, 123.5, 129.5, 131.2, 157.1
CdLI ₂ (L = 4)	66.9	47.5, 47.8	25.5, 25.3	111.3, 120.1, 125.3, 128.8, 131.0, 156.7
ligand 7	66.2	54.5, 56.5	25.4, (40.5, NCH ₃)	111.0, 119.4, 125.3, 127.2, 131.7, 156.9
ZnLI ₂ (L = 7)	66.3	56.4, 54.3	23.9, (40.5, NCH ₃)	111.2, 119.7, 123.5, 129.2, 132.2, 157.0

^a In ppm relative to tetramethylsilane. ^b In all cases the splitting patterns observed in the corresponding off-resonance spectra were in accord with the proposed structures. ^c These resonances in the corresponding ligand containing a bromo substituent in each aromatic ring [on C(4) from the ring carbon bound to oxygen] are δ 47.9 and 49.5. The induced shifts caused by the bromo substituents relative to the resonances of 2 suggest that the higher chemical shift resonance is correctly assigned to the methylene carbon adjacent to the aromatic ring. ^d b = broad.

regard that certain cyclic polyethers have been reported to show no measurable affinity for zinc and cadmium in polar solvents^{24,25} (even though solid adducts of crowns with zinc and cadmium salts have been reported to precipitate under anhydrous conditions from reaction solutions of low polarity²⁶). A parallel study of the ¹³C NMR spectra of the free ligands and selective complexes did not show any well-defined trends in the chemical shifts of the individual resonances—a result which is perhaps ascribable to the tendency of ¹³C resonances to be more susceptible to conformational influences than to “external” perturbations (such as solvation effects or electronic effects resulting from complexation to a diamagnetic ion).²⁷ The ¹H and ¹³C NMR chemical shift data are tabulated in Tables V and VI.

The NMR studies thus confirm that coordination of the nitrogen atoms of the respective macrocycles to zinc and cadmium occurs in solution, while the question of coordination of the ether oxygens must remain open. For investigation of

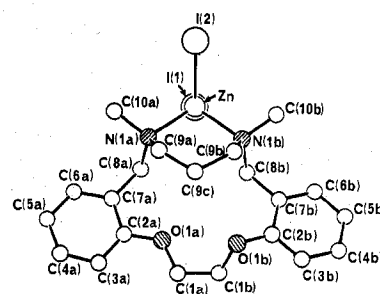


Figure 2. Zinc(II) iodide complex of the 15-membered macrocycle 7 viewed down the Zn-I(1) bond, with atom labels as used in Tables I, II, and VII.

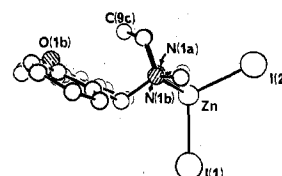


Figure 3. Side view of ZnLI₂ (L = 7) showing the configurations of the 6- and 13-membered chelate rings defined by the macrocycle.

details of the coordination in the solid state, an X-ray diffraction study of one such complex, ZnLI₂ (L = 7), has been undertaken.

- (24) Izatt, R. M.; Terry, R. E.; Haymore, B. L.; Hansen, L. D.; Dalley, N. K.; Avondet, A. G.; Christensen, J. J. *J. Am. Chem. Soc.* **1976**, *98*, 7620.
 Izatt, R. M.; Terry, R. E.; Nelson, D. P.; Chan, Y.; Eatough, D. J.; Bradshaw, J. S.; Hansen, L. D.; Christensen, J. J. *Ibid.* **1976**, *98*, 7626.
 (25) Izatt, R. M.; Eatough, D. J.; Christensen, J. J. *Struct. Bonding (Berlin)* **1973**, *16*, 166.
 (26) Wulfsberg, G.; Weiss, A. *J. Chem. Soc., Dalton Trans.* **1977**, 1640 and references therein.
 (27) Live, D.; Chan, S. I. *J. Am. Chem. Soc.* **1976**, *98*, 3769 and references therein.

Table VII. Interatomic Bond Lengths and Angles

Bond Lengths (Å)			
Zn-I(1)	2.552 (2)	Zn-I(2)	2.569 (2)
Zn-N(1a)	2.108 (11)	Zn-N(1b)	2.107 (10)
C(1a)-O(1a)	1.31 (2)	C(1b)-O(1b)	1.34 (2)
O(1a)-C(2a)	1.35 (2)	O(1b)-C(2b)	1.36 (2)
C(2a)-C(3a)	1.38 (2)	C(2b)-C(3b)	1.37 (2)
C(3a)-C(4a)	1.41 (2)	C(3b)-C(4b)	1.38 (2)
C(4a)-C(5a)	1.33 (2)	C(4b)-C(5b)	1.36 (2)
C(5a)-C(6a)	1.41 (2)	C(5b)-C(6b)	1.40 (2)
C(6a)-C(7a)	1.39 (2)	C(6b)-C(7b)	1.38 (2)
C(7a)-C(2a)	1.39 (2)	C(7b)-C(2b)	1.39 (2)
C(7a)-C(8a)	1.52 (2)	C(7b)-C(8b)	1.52 (2)
C(8a)-N(1a)	1.51 (2)	C(8b)-N(1b)	1.52 (2)
N(1a)-C(9a)	1.49 (2)	N(1b)-C(9b)	1.48 (2)
N(1a)-C(10a)	1.52 (2)	N(1b)-C(10b)	1.51 (2)
C(9a)-C(9c)	1.48 (2)	C(9b)-C(9c)	1.55 (2)
C(1a)-C(1b)	1.46 (2)		

Angles (Deg)			
N(1a)-Zn-I(1)	111.8 (3)	N(1b)-Zn-I(1)	109.3 (3)
N(1a)-Zn-I(2)	107.9 (3)	N(1b)-Zn-I(2)	110.0 (3)
N(1a)-Zn-N(1b)	101.5 (4)	I(1)-Zn-I(2)	115.3 (1)
C(1b)-C(1a)-O(1a)	113 (1)	C(1a)-C(1b)-O(1b)	115 (1)
C(1a)-O(1a)-C(2a)	123 (1)	C(1b)-O(1b)-C(2b)	119 (1)
O(1a)-C(2a)-C(3a)	123 (1)	O(1b)-C(2b)-C(3b)	119 (1)
O(1a)-C(2a)-C(7a)	116 (1)	O(1b)-C(2b)-C(7b)	121 (1)
C(3a)-C(2a)-C(7a)	122 (2)	C(3b)-C(2b)-C(7b)	120 (2)
C(2a)-C(3a)-C(4a)	117 (2)	C(2b)-C(3b)-C(4b)	121 (2)
C(3a)-C(4a)-C(5a)	123 (2)	C(3b)-C(4b)-C(5b)	119 (2)
C(4a)-C(5a)-C(6a)	119 (2)	C(4b)-C(5b)-C(6b)	120 (2)
C(5a)-C(6a)-C(7a)	120 (2)	C(5b)-C(6b)-C(7b)	120 (2)
C(6a)-C(7a)-C(2a)	119 (1)	C(6b)-C(7b)-C(2b)	119 (1)
C(6a)-C(7a)-C(8a)	120 (1)	C(6b)-C(7b)-C(8b)	120 (1)
C(2a)-C(7a)-C(8a)	120 (1)	C(2b)-C(7b)-C(8b)	121 (1)
C(7a)-C(8a)-N(1a)	117 (1)	C(7b)-C(8b)-N(1b)	116 (1)
C(8a)-N(1a)-Zn	108.6 (8)	C(8b)-N(1b)-Zn	110.2 (7)
C(8a)-N(1a)-C(9a)	114 (1)	C(8b)-N(1b)-C(9b)	113 (1)
C(8a)-N(1a)-C(10a)	110 (1)	C(8b)-N(1b)-C(10b)	109 (1)
C(9a)-N(1a)-Zn	106.6 (8)	C(9b)-N(1b)-Zn	107.3 (8)
C(9a)-N(1a)-C(10a)	108 (1)	C(9b)-N(1b)-C(10b)	110 (1)
C(10a)-N(1a)-Zn	109.7 (8)	C(10b)-N(1b)-Zn	107.4 (8)
N(1a)-C(9a)-C(9c)	118 (1)	N(1b)-C(9b)-C(9c)	116 (1)
C(9a)-C(9c)-C(9b)	118 (1)		

X-ray Structure of $ZnLI_2$ ($L = 7$). The structure determination demonstrates that in this complex the ether oxygen atoms are not coordinated and the zinc ion lies outside the macrocycle cavity (Figure 2). In order to achieve this mode of coordination to the zinc, the macrocycle adopts a different configuration from those observed^{4,6} previously in complexes of the related 15-membered ring **2**. The 6-membered chelate ring has the expected chair configuration, but with the central methylene carbon atom C(9c) lying over the cavity defined by the donor atoms (Figure 3). The remaining part of the inner great ring of the macrocycle and the fused benzene rings lies approximately in the same plane (see Figure 3). The atoms O(1a), O(1b), C(1a), and C(1b) have highly anisotropic thermal parameters (Table II) with an elongation of the thermal ellipsoids in a direction which is consistent with thermal motion or disorder perpendicular to the plane of the macrocycle.

The zinc atom has an approximately tetrahedral coordination geometry with Zn-I and Zn-N bond lengths (Table VII) close to the ranges (2.53–2.56 and 2.04–2.13 Å, respectively)^{28,29} found in related tetrahedral complexes with “ N_2I_2 ” donor sets.

It is of interest that the 1,3-diaminopropane unit in the complex $ZnLI_2$ ($L = 7$) defines a very similar coordination

Table VIII. Comparison of log (stability constants)^a for Complexation of Cobalt, Nickel, Copper, and Zinc with Macrocycles 1–4: $M^{2+} + L \rightleftharpoons ML^{2+}$

macrocycle	ring size	M			
		Co	Ni ^b	Cu ^c	Zn
1	14		3.7	8.2	~3.0
2	15	<4.5	5.4	7.2	4.1 ^{d,e}
3	16	<4.5	5.8	7.7	4.3 ^d
4	17	<4.5	~3.5	7.2	4.1 ^d

^a 25 °C; in 95% methanol [$I = 0.1$, $(CH_3)_4NCl$]. ^b From ref 5. ^c From ref 6. ^d Standard deviation ± 0.1 . ^e The corresponding log value for the zinc complex of ligand 6 is 3.8 ± 0.1 .

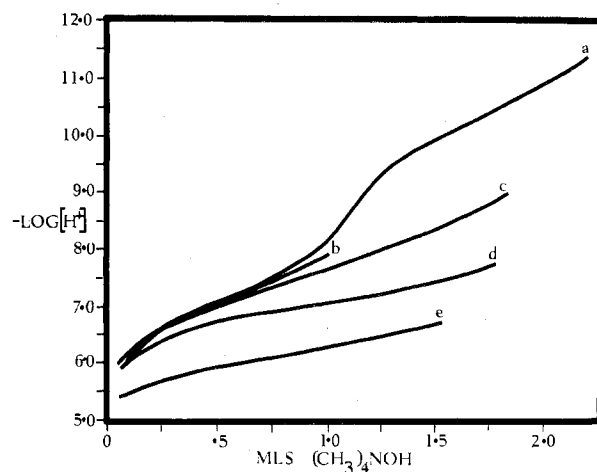
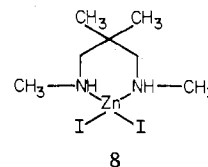


Figure 4. Potentiometric titration curves: (a) LH_2^{2+} ($L = 3$); (b) $Co^{2+} + LH_2^{2+}$ ($L = 3$); (c) $Zn^{2+} + LH_2^{2+}$ ($L = 3$); (d) $Ni^{2+} + LH_2^{2+}$ ($L = 3$); (e) $Cu^{2+} + LH_2^{2+}$ ($L = 3$). Concentrations of both LH_2^{2+} and M^{2+} were 2.0×10^{-3} M in all cases, and 50 mL of 95% methanol solution [$I = 0.1$, $(CH_3)_4NCl$] was used for the titration. $(CH_3)_4NOH$ (0.096 M) in 95% methanol was used as titrant.

geometry at the zinc ion to that observed²⁹ in the “simple” chelate **8**. This suggests that the rest of the macrocycle is



sufficiently flexible to allow the 1,3-diaminopropane unit to adopt an arrangement close to the optimum geometry for forming a tetrahedral metal complex. On the basis of the NMR and conductance data discussed previously it seems likely that each of the other zinc and cadmium complexes of the ligands 1–7 has an approximately tetrahedral geometry.

Stability Constant Determinations. The log K values for the cobalt(II) and zinc(II) complexes of the unsubstituted 14- to 17-membered macrocycles were investigated by using the potentiometric procedure used previously to study the interaction of these ligands with nickel and copper.^{5,6} In no case could the entire titration curve be obtained, owing to precipitation and/or hydrolysis occurring as the pH was raised. For cobalt, such early precipitation together with the relatively low log K values with this ion resulted in no reliable values being obtained; precipitation occurred before \bar{n} values (\bar{n} is the mean number of ligands coordinated per metal ion) of 0.1 were reached in all cases. In contrast, for zinc, maximum \bar{n} values of 0.23, 0.57, 0.47, and 0.64 were achieved for the complexes of **1–4**, respectively. In accord with the NMR titration results, the potentiometric data for zinc complexation refined satisfactorily with the assumption of the presence of only 1:1

- (28) Htoon, S.; Ladd, M. F. C. *J. Cryst. Mol. Struct.* **1974**, *4*, 357. Le Querler, J. F.; Borel, M. M.; LeClaire, A. *Acta Crystallogr., Sect. B* **1977**, *B33*, 2299. Sergienko, V. S.; Porai-Koshits, M. A.; Rubinchik, B. Y.; Bukman, L. A.; Tsintsadze, G. V. *Koord. Khim.* **1978**, *4*, 1760.
 (29) Richard, P.; Boulanger, A.; Guedon, J.-F.; Kasowski, W. J.; Bordeleau, C. *Acta Crystallogr., Sect. B* **1977**, *B33*, 1310.

(metal:ligand) species, and no improvement occurred when other species were included. All equilibria were established quickly.

A listing of the respective log *K* values together with the previously determined values for nickel and copper are given in Table VIII, and a representative set of potentiometric curves (for the complexes of 3) are reproduced in Figure 4. In general, the log *K* values follow the expected Irving-Williams³⁰ order of Co(II) < Ni(II) < Cu(II) > Zn(II).

As mentioned previously, with nickel(II) the stability reaches a peak for the 16-membered ring complex. From consideration of the X-ray structures of the nickel complexes of 2 and 3 together with the literature values for typical nickel-ether oxygen and nickel-nitrogen bond distances, it seems likely that the 16-membered macrocycle provides the ring of least strain for the nickel ion.^{3,5} For copper and zinc, the absence of a definite peak in the respective log *K* values can be rationalized in terms of the proposed solution structures of these complexes. For copper, the metal ion is very likely not completely encircled by the donor atoms of the respective macrocycles, and, indeed, different coordination geometries may well occur along the series of complexes.⁶ For zinc, the evidence discussed above

suggests that the ether oxygen donors of each macrocycle do not coordinate. Thus for both these metal-ion systems no clear ring-size discrimination effects would be expected and none are observed.

Acknowledgment. L.F.L. expresses thanks to Professor G. Anderegg (ETH, Zürich) and Dr. J. T. Baker (Roche Research Institute of Marine Pharmacology, Sydney) for assistance. Acknowledgment is made to the Australian Research Grants Committee for support and the Australian Institute of Nuclear Science and Engineering for a travel grant. M.M. and P.A.T. thank the Science Research Council (U.K.) for diffractometer equipment and computing facilities.

Registry No. 1, 65639-47-6; 2, 65639-43-2; 3, 65639-49-8; 4, 66793-29-1; 7, 66793-30-4; Co(L₂)(SCN)₂, 74381-17-2; Co(L₂)Br₂, 74381-18-3; Co(L₃)(SCN)₂, 74381-19-4; Co(L₄)(SCN)₂, 74381-20-7; Co(L₄)Br₂, 74381-21-8; Co(L₄)Cl₂, 74381-22-9; Zn(L₁)I₂, 74381-23-0; Cd(L₁)I₂, 74381-24-1; Zn(L₂)I₂, 74381-25-2; Cd(L₂)I₂, 74381-26-3; Zn(L₃)I₂, 74381-27-4; Cd(L₃)I₂, 74381-28-5; Zn(L₄)I₂, 74381-29-6; Cd(L₄)I₂, 74381-30-9; Zn(L₇)I₂, 74381-31-0; Zn(L₂)Cl₂, 74381-32-1; Zn(L₄)Cl₂, 74381-33-2; Zn(L₅)I₂, 74397-15-2; Zn(L₆)I₂, 74397-16-3; Zn(L₇)Cl₂, 74381-34-3; Cd(L₅)I₂, 74381-35-4; Cd(L₆)I₂, 74397-17-4.

Supplementary Material Available: Listings of analytical data for the complexes and structure factor tables for the X-ray structure determination of ZnLI₂ (L = 7) (10 pages). Ordering information is given on any current masthead page.

(30) Irving, H.; Williams, R. J. P. *J. Chem. Soc.* 1953, 3192.

Contribution from the Department of Chemistry,
Washington State University, Pullman, Washington 99164

Kinetics and Mechanism of the Reaction of Palladium(II) Complexes of *o*-(Diphenylphosphino)thioanisole and *o*-(Diphenylphosphino)selenoanisole with Nucleophiles Thiocyanate and Iodide. Carbon-13 NMR Spectroscopy of the Methyl-Heteroatom Complexes and X-ray Structural Characterization of Diiodobis[*o*-(diphenylphosphino)benzenethiolato]dipalladium(II)¹

D. MAX ROUNDHILL,* STEPHANIE G. N. ROUNDHILL, WILLIAM B. BEAULIEU,
and UTTARAYAN BAGCHI

Received April 23, 1980

The kinetics of the reaction of the nucleophiles thiocyanate and iodide with complexes PdX₂(*o*-MeSC₆H₄PPh₂) (X = SCN, I) show a rate law rate = *k*₂[PdX₂(*o*-MeSC₆H₄PPh₂)] [X⁻]. Second-order rate constants *k*₂ for the thiocyanate reaction have been measured, and the activation parameters Δ*H*[‡] and Δ*S*[‡] are 22.9 ± 1.0 kcal/mol and -9.2 ± 2.1 cal/mol. For the selenium analogue complex these respective values are 18.9 ± 1.3 kcal/mol and -12.9 ± 2.3 cal/mol. With iodide as nucleophile an equilibrium condition is established. Rates are calculated from the data both for the demethylation and for the reverse addition of methyl iodide. The alkylation reaction is approximately 50 times faster. The product from the iodide demethylation reaction is considered to be the anion [PdI₂(*o*-SC₆H₄PPh₂)]⁻ on the basis of visible spectroscopy. The mechanism of the nucleophile-induced demethylation reaction resembles the Zeisel ether cleavage.

¹H and ¹³C NMR parameters have been measured and compared both for the free ligands *o*-MeSC₆H₄PPh₂, *o*-MeSeC₆H₄PPh₂, *o*-MeOC₆H₄PPh₂, and *o*-Me₂NC₆H₄PPh₂ and for a series of transition-metal complexes of these ligands. Complexation causes a small downfield shift in the position of the ¹H NMR resonance of the methyl group and a larger downfield shift in the ¹³C NMR parameter. These data show that complexation of the heteroatom causes an increased carbonium ion character at the methyl carbon.

New complexes RuCl₂(*o*-MeSC₆H₄PPh₂)₂ and RuCl₂(*o*-MeSeC₆H₄PPh₂)₂ have been prepared with the S and Se atoms complexed to Ru(II). The mixed ligand *o*-MeSeC₆H₄SMe

forms a chelate complex PdCl₂(*o*-MeSeC₆H₄SMe). ¹H, ¹³C, and ⁷⁷Se NMR spectra of this ligand are measured and compared with the ¹H and ¹³C NMR spectra of the palladium complex.

The compound [PdI(*o*-SC₆H₄PPh₂)₂]₂, obtained from thermolysis of PdI₂(*o*-MeSC₆H₄PPh₂), crystallizes with 4 molecules per unit cell in a *P* $\bar{1}$ space group. Cell parameters are *a* = 19.870 (6) Å, *b* = 14.754 (5) Å, *c* = 14.856 (6) Å, cos α = -0.2643 (6), cos β = -0.2226 (4), and cos γ = 0.0089 (4). Refinement of the structure to *R* = 0.056 shows two dimeric molecules with Pd-Pd separations of 2.964 and 2.916 Å and S-S separations of 2.972 and 3.006 Å. The molecules are bridged by double thiolato bridges, and the folding along the S-S line leads to dihedral angles of 74.3 and 79.8°. The Pd₂S₂ rhombus is unsymmetrical with the Pd-S bonds trans to the phosphorus atom being slightly longer than those trans

(1) A preliminary communication of this work has been published: Roundhill, D. M.; Beaulieu, W. B.; Bagchi, U. *J. Am. Chem. Soc.* 1979, 101, 5428.